Title	Exact wave propagation in a spacetime with a cosmic string
Author(s)	Suyama, T; Tanaka, T; Takahashi, R
Citation	PHYSICAL REVIEW D (2006), 73(2)
Issue Date	2006-01
URL	http://hdl.handle.net/2433/49933
Right	Copyright 2006 American Physical Society
Type	Journal Article
Textversion	publisher

PHYSICAL REVIEW D **73,** 024026 (2006)

Exact wave propagation in a spacetime with a cosmic string

Teruaki Suyama,[1] Takahiro Tanaka,[1] and Ryuichi Takahashi[2]
[1]*Department of Physics, Kyoto University, Kyoto 606-8502, Japan*
[2]*Division of Theoretical Astrophysics, National Astronomical Observatory of Japan, Mitaka, Tokyo 181-8588, Japan*
(Received 11 December 2005; published 31 January 2006)

We present exact solutions of the massless Klein-Gordon equation in a spacetime in which an infinite straight cosmic string resides. The first solution represents a plane wave entering perpendicular to the string direction. We also present and analyze a solution with a static pointlike source. In the short wavelength limit these solutions approach the results obtained by using the geometrical optics approximation: magnification occurs if the observer lies in front of the string within a strip of angular width $8\pi G\mu$, where μ is the string tension. We find that when the distance from the observer to the string is less than $10^{-3}(G\mu)^{-2}\lambda \sim 150\ \mathrm{Mpc}(\lambda/\mathrm{AU})(G\mu/10^{-8})^{-2}$, where λ is the wavelength, the magnification is significantly reduced compared with the estimate based on the geometrical optics due to the diffraction effect. For gravitational waves from neutron star (NS)-NS mergers the several lensing events per year may be detected by DECihertz interferometer gravitational wave observatory (DECIGO)/big bang observer (BBO).

DOI: 10.1103/PhysRevD.73.024026 PACS numbers: 04.30.Nk, 98.80.Cq

I. INTRODUCTION

Typical wavelength of gravitational waves from astrophysical compact objects such as black hole (BH)-BH binaries is in some cases very long so that wave optics must be used instead of geometrical optics when we discuss gravitational lensing. More precisely, if the wavelength becomes comparable or longer than the Schwarzschild radius of the lens object, the diffraction effect becomes important and as a result the magnification factor approaches unity [1–5]. Mainly due to the possibility that the wave effects could be observed by future gravitational wave observations, several authors [6–15] have studied wave effects in gravitational lensing in recent years.

In most of the works which studied gravitational lensing phenomenon in the framework of wave optics, isolated and normal astronomical objects such as galaxies are concerned as lens objects. Recently Yamamoto and Tsunoda [12] studied wave effects in gravitational lensing by an infinite straight cosmic string. The metric around a cosmic string is completely different from that around a usual massive object.

Cosmic strings generically arise as solitons in a grand unified theory and could be produced in the early Universe as a result of symmetry breaking phase transition [16,17]. If symmetry breaking occurred after inflation, the strings might survive until the present Universe. Recently, cosmic strings attract a renewed interest partly because a variant of their formation mechanism was proposed in the context of the brane inflation scenario [18–24]. In this scenario inflation is driven by the attractive force between parallel D-branes and parallel anti-D-branes in a higher-dimensional spacetime. When those brane-antibrane pairs collide and annihilate at the end of inflation, lower-dimensional D-branes, which behave like monopoles, cosmic strings or domain walls from the view point of four-dimensional observers, are formed generically [25–29].

For some time, cosmic string was a candidate for the seed of structure formation of our Universe, but this possibility was ruled out by the measurements of the spectrum of cosmic microwave background (CMB) anisotropies [30,31]. The current upper bound on the dimensionless string tension $G\mu$ is around $10^{-7} \sim 10^{-6}$, which comes from the observations of CMB [32–35] and/or the pulsar timing [36–39]. Although cosmic string cannot occupy dominant fraction of the energy density of the Universe, its non-negligible population is still allowed observationally [40,41]. In fact, Sazhin *et al.* [42,43] reported that CSL-1, which is a double image of elliptical galaxies with angular separation 1.9 arcsec, could be the first case of the gravitational lensing by a cosmic string with $G\mu \approx 4 \times 10^{-7}$.

We study in detail wave effects in the gravitational lensing by an infinite straight cosmic string. In Ref. [12], wave propagation around a cosmic string was studied but they put the wave form around the string by hand.[1] Their prescription is correct only in the limit of geometrical optics, which breaks down when the wavelength becomes longer than a certain characteristic length. In this paper, we present exact solutions of the (scalar) wave equation in a

[1]After submitting this paper, we have noticed a paper [44] in which the solutions of the wave equations around the cosmic string are given, though the apparent expressions are different from those given in this paper. In [44] the author estimated the amplitude of the diffracted wave to be suppressed by $\mathcal{O}(G\mu)$ compared with that corresponding to the geometrical optics. We show that the importance of the diffraction effects are determined by the combination of three parameters, $G\mu$, the distance from the string to the observer and the wavelength, and that the relative amplitude of the diffracted wave can be $\mathcal{O}(1)$ for realistic astrophysical situations.

spacetime with a cosmic string. We analytically show that our solutions reduce to the results of the geometrical optics in the short wavelength limit. We derive a simple analytic formula of the leading order corrections to the geometrical optics due to the finite wavelength effects and also an expression for the long wavelength limit. Interference caused by the lensing remains due to the diffraction effects even when only a single image can be seen in the geometrical optics. This fact increases the lensing probability by cosmic strings.

This paper is organized as follows. In Section II, we construct a solution of the wave equation on a background spacetime with an infinite straight cosmic string in the case that a source of the wave is located infinitely far. An extension to the case in which a point source is located at a finite distance is given in Appendix B. In Section III, we study properties of the solution obtained in Section II in detail. In Section IV, we focus on compact binaries as the sources of gravitational waves and discuss the possible effects due to finiteness of the lifetime and the frequency evolution of the binaries on the detection of the gravitational waves which pass near a cosmic string. We also give a rough estimate for the event rate of the lensing of gravitational waves from neutron star (NS)-NS mergers assuming DECihertz interferometer gravitational wave observatory (DECIGO)/big bang observer (BBO). Section V is devoted to summary.

II. A SOLUTION OF THE WAVE EQUATION AROUND AN INFINITE STRAIGHT COSMIC STRING

A solution of Einstein equations around an infinite straight cosmic string to first order in $G\mu$ is given by [45]

$$d^2s = -dt^2 + dr^2 + (1-\Delta)^2 r^2 d\theta^2 + dz^2, \qquad (1)$$

where (r, z, θ) is a cylindrical coordinate $(0 \le \theta < 2\pi)$ and $2\pi\Delta \approx 8\pi G\mu$ is the deficit angle around the cosmic string. Spatial part of the above metric describes the Euclidean space with a wedge of angular size $2\pi\Delta$ removed. Because of the deficit angle around a string, double images of the source are observed with an angular separation $\lesssim 2\pi\Delta$ when a source is located behind the string in the limit of geometrical optics. In general for a wave with a finite wavelength, some interference pattern appears. An exact solution of Einstein equations around a finite thickness string has been already obtained [46], but we use the metric (1) as a background since the string thickness is negligibly small compared with the Einstein radius, $\approx \pi D\Delta$, where D is the distance from the observer to the string.

Throughout the paper, we consider waves of a massless scalar field instead of gravitational waves for simplicity, but the wave equations are essentially the same in these two cases. An extension to the cosmological setup is straightforwardly done by adding an overall scale factor. In that case the time coordinate t is to be understood as the conformal time. The wave equation remains unchanged if we consider a conformally coupled field, but it is modified for the other cases due to curvature scattering. The correction due to curvature scattering of the Friedmann Universe is suppressed by the square of the ratio between the wavelength and the Hubble length, which can be neglected in any situations of our interest.

Our goal of this section is to construct a solution of the wave equation which corresponds to a plane wave injected perpendicularly to and scattered by the cosmic string. This situation occurs if the distance between the source and the string is infinitely large. In order to construct such a solution, we introduce a monochromatic source uniformly extended in the z-direction and localized in r-θ plane,

$$S = \frac{B}{(1-\Delta)}\delta(r - r_o)\delta(\theta - \pi)e^{-i\omega t}, \qquad (2)$$

where ω is the frequency and we have introduced B, a constant independent of Δ, to adjust the overall normalization when we later take the limit $r_o \to \infty$. The factor $(1-\Delta)^{-1}$ appears because θ-coordinate used in the metric (1) differs from the usual angle

$$\varphi \equiv (1-\Delta)\theta. \qquad (3)$$

Here we consider a uniformly extended source instead of a point source since the former is easier to handle. When the limit $r_o \to \infty$ is taken, the answers are identical in these two cases. The case with a pointlike source at a finite distance is more complicated. This case is treated in Appendix B.

Now the wave equation that we are to solve is

$$\left(\frac{\partial^2}{\partial r^2} + \frac{1}{r}\frac{\partial}{\partial r} + \frac{1}{(1-\Delta)^2 r^2}\frac{\partial^2}{\partial\theta^2} + \omega^2\right)\phi(r,\theta) = \frac{B}{1-\Delta}\delta(r - r_o)\delta(\theta - \pi). \qquad (4)$$

Since $\phi(r, -\theta)$ satisfies the same Eq. (4) as $\phi(r, \theta)$ does, $\phi(r, \theta)$ is even in θ. Thus, it can be expanded as

$$\phi(r,\theta) = \sum_{m=0}^{\infty} f_m(r)\cos m\theta. \qquad (5)$$

From Eqs. (4) and (5), the equations for $f_m(r)$ are

$$\left(\frac{d^2}{dr^2} + \frac{1}{r}\frac{d}{dr} + \omega^2 - \frac{\nu_m^2}{r^2}\right)f_m(r) = \epsilon_m \frac{(-1)^m}{1-\Delta}\frac{B}{2\pi}\delta(r - r_o), \qquad (6)$$

where $\epsilon_o \equiv 1$, $\epsilon_m \equiv 2 (m \ge 1)$, and $\nu_m \equiv (1-\Delta)^{-1}m$. The solution of Eq. (6) except for $r = r_o$ is a linear combination of Bessel function and Hankel function. We impose that the wave ϕ is regular at $r = 0$ and pure outgoing at infinity. Further, imposing that the wave is continuous at $r = r_o$, $f_m(r)$ becomes

$$f_m(r) = N_m(H^{(1)}_{\nu_m}(\omega r_o)J_{\nu_m}(\omega r)\Theta(r_o - r) + J_{\nu_m}(\omega r_o)H^{(1)}_{\nu_m}(\omega r)\Theta(r - r_o)), \quad (7)$$

where $\Theta(x)$ is the Heaviside step function. Substituting Eq. (7) into Eq. (6), the normalization factor N_m is determined as

$$N_m = \frac{B}{1-\Delta}\frac{\epsilon_m(-1)^m}{2\pi\omega}[J_{\nu_m}(\omega r_o)H^{(1)\prime}_{\nu_m}(\omega r_o) - H^{(1)}_{\nu_m}(\omega r_o)J'_{\nu_m}(\omega r_o)]^{-1} = \frac{Br_0\epsilon_m(-1)^m}{4i(1-\Delta)}, \quad (8)$$

where $'$ denotes a differentiation with respect to the argument. From Eqs. (7) and (8) with the aid of the asymptotic formulae of the Bessel and Hankel functions, $\phi(r, \theta)$ for $r_o \to \infty$ can be written as

$$\phi(r,\theta) = \frac{-iB}{2\sqrt{2}(1-\Delta)}\sqrt{\frac{r_o}{\pi\omega}}e^{i\omega r_o - i(\pi/4)} \times \sum_{m=0}^{\infty}\epsilon_m i^m e^{-(im\pi\Delta)/[2(1-\Delta)]}J_{\nu_m}(\omega r)\cos m\theta. \quad (9)$$

We determine the overall normalization of the source amplitude B, independently of $G\mu$, so that Eq. (9) becomes a plane wave $e^{i\omega r\cos\theta}$ when $G\mu = 0$. This condition leads to $B = -2\sqrt{\frac{2\pi\omega}{r_o}}e^{-i\omega r_o - i\pi/4}$. Then, finally ϕ becomes

$$\phi(r,\theta) = \frac{1}{1-\Delta}\sum_{m=0}^{\infty}\epsilon_m i^m e^{-(im\Delta\pi)/[2(1-\Delta)]}J_{\nu_m}(\omega r) \times \cos m\theta. \quad (10)$$

III. LIMITING BEHAVIORS OF THE SOLUTION

A. Approximate wave form in the wave zone

The solution (10) describes the wave form propagating around a cosmic string. But it is not easy to understand the behavior of the solution because it is given by a series. In fact, it takes much time to perform the summation in Eq. (10) numerically for a realistic value of tension of the string, say, $G\mu \lesssim 10^{-6}$ because of slow convergence of the series. In particular it is not manifest whether the amplification of the solution in the short wavelength limit coincides with the one which is obtained by the geometrical optics approximation. Therefore it will be quite useful if one can derive a simpler analytic expression. Here we reduce the formula by assuming that the distance between the string and the observer is much larger than the wavelength,

$$\xi \equiv \omega r \gg 1, \quad (11)$$

which is valid in almost all interesting cases.

Using an integral representation of the Bessel function,

$$J_\nu(\xi) = \frac{1}{2i\pi}\int_C dt\, e^{\xi\sinh t - \nu t}, \quad (12)$$

where the contour of the integral C is such as shown in Fig. 1, Eq. (10) can be written as

$$\phi(\xi,\theta) = -\frac{J_0(\xi)}{1-\Delta} + \frac{1}{1-\Delta}\frac{1}{2i\pi}\int_C dt\, e^{\xi\sinh t} \times \sum_{m=0}^{\infty} e^{-[mt/(1-\Delta)]+[(\pi/2)mi]-[(im\pi\Delta)/2(1-\Delta)]} \times (e^{im\theta} + e^{-im\theta}). \quad (13)$$

When t is in the segment of the integration contour C along the imaginary axis, the summation over m does not converge because the absolute value of each term in the summation is all unity. In order to make the series to converge, we need to think that the integration contour C is not exactly on the imaginary axis but t always has a positive real part. For bookkeeping purpose, we multiply each term in the sum by a factor $e^{-\epsilon m}$ (ϵ is an infinitesimally small positive real number). Then Eq. (13) becomes

$$\phi(\xi,\theta) = -\frac{J_0(\xi)}{1-\Delta} + \psi(\xi,\theta) + \psi(\xi,-\theta), \quad (14)$$

where $\psi(\xi,\theta)$ is defined by

$$\psi(\xi,\theta) := \frac{1}{1-\Delta}\frac{1}{2i\pi}\int_C dt\frac{e^{\xi\sinh t}}{1-e^{-(t-t_*)/(1-\Delta)}}, \quad (15)$$

with

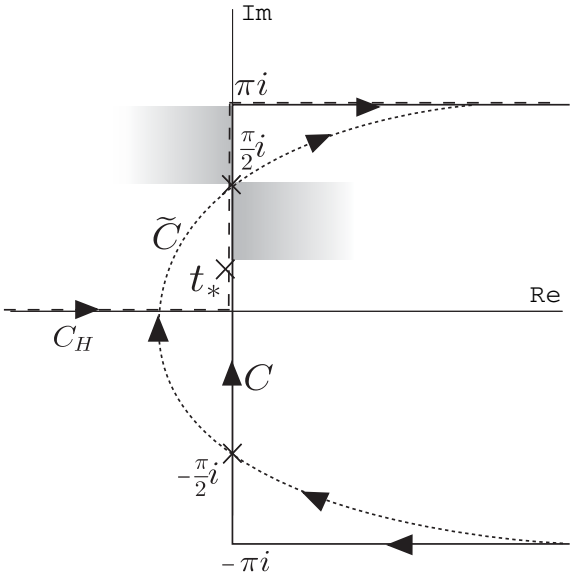

FIG. 1. Black, dotted, and dashed lines are contours of the integral C, $\tilde{C}$, and C_H, respectively. $\pm i\frac{\pi}{2}$ are the saddle points of $e^{\xi\sinh t}$.

$$t_* := -\epsilon + i\frac{\pi}{2} - i\frac{\alpha(\theta)}{\sqrt{\xi}}, \tag{16}$$

and $\alpha(\theta) := (\pi\Delta - (1-\Delta)\theta)\sqrt{\xi}$.

Now we find that all we need to evaluate is $\psi(\xi, \theta)$ in order to obtain an approximate formula for $\phi(\xi, \theta)$. This integral will not be expressed by simple known functions in general, but the integration can be performed by using the method of steepest descent in the limit $\xi \gg 1$.

The integrand of Eq. (15) has two saddle points located at $t = t_+ \approx i\pi/2$ and $t = t_- \approx -i\pi/2$ in the vicinity of the integration contour C. We should also notice that the integrand has a pole at $t = t_*$, which is also infinitesimally close to the contour of the integral C. This pole is located near the saddle point at $t = t_+$ as far as Δ and θ are small. Hence the treatment of the saddle point at $t = t_+$ is much more delicate than that of the saddle point at $t = t_-$. We only discuss the saddle point at $t = t_+$, then the case at $t = t_-$ is a trivial extension.

When $\Re(t) > 0,\ \Im(t) < i\frac{\pi}{2}$ or $\Re(t) < 0,\ \Im(t) > i\frac{\pi}{2}$, which corresponds to shaded regions in Fig. 1, $e^{\xi \sinh t}$ diverges in the limit $\xi \to \infty$. If $\alpha(\theta) > 0$, the pole at $t = t_*$ is in the bottom-left unshaded region. In this case we cannot deform the contour to the direction of the steepest descent at $t = t_+$ without crossing the pole at $t = t_*$. The deformed contour which is convenient to apply the method of the steepest descent is such that is shown as $\tilde{C}$ in Fig. 1. When we deform the integration contour from C to $\tilde{C}$, there arises an additional contribution corresponding to the residue at $t = t_*$ when $\alpha(\theta) > 0$. On the other hand, if $\alpha(\theta) < 0$, the pole is in the top-left shaded region. In this case, we can deform the contour of the integral to the direction of the steepest descent without crossing the pole t_*. Hence no additional term arises.

From these observations, we find that it is necessary to evaluate the integral (15) separately depending on the signature of $\alpha(\theta)$. Though the calculation itself can be done straightforwardly, it is somewhat complicated because the saddle point and the pole are close to each other. When the pole is located inside the region around the saddle point that contributes dominantly to the integral, a simple Gaussian integral does not give a good approximation. Detailed discussions about this point are given in Appendix A. Here we only quote the final result which keeps terms up to $O(1/\sqrt{\xi})$,

$$\begin{aligned}\psi(\xi, \theta) \approx{}& \exp\left(i\xi\cos\frac{\alpha(\theta)}{\sqrt{\xi}}\right)\Theta(\alpha(\theta)) - \frac{\sigma(\theta)}{\sqrt{\pi}} \\ &\times \exp\left(i\xi + \frac{i\alpha(\theta)}{(1-\Delta)\sqrt{\xi}} - \frac{i}{2}\tilde{\alpha}^2(\theta)\right) \\ &\times \mathrm{Erfc}\left(\sigma(\theta)\frac{\tilde{\alpha}(\theta)}{\sqrt{2}}e^{-i\pi/4}\right) \\ &+ \frac{1}{\sqrt{2\pi\xi}}\frac{1}{1-\Delta}\frac{e^{-i\xi+i\pi/4}}{1 - e^{\frac{i}{1-\Delta}(\pi - \alpha(\theta)/\sqrt{\xi})}},\end{aligned} \tag{17}$$

where

$$\tilde{\alpha}(\theta) := i(1-\Delta)\sqrt{\xi}\left[1 - \exp\left(i\frac{\alpha(\theta)}{(1-\Delta)\sqrt{\xi}}\right)\right], \tag{18}$$

$$\sigma(\theta) := \mathrm{sign}(\alpha(\theta)), \tag{19}$$

and

$$\mathrm{Erfc}\,(x) := \int_x^{+\infty} dt\, e^{-t^2}. \tag{20}$$

We are mostly interested in the cases with $\Delta, \theta \ll 1$. Then, we have $\alpha(\theta)/\sqrt{\xi} \ll 1$, and therefore $\tilde{\alpha}(\theta)$ reduces to $\alpha(\theta)$. The second term in Eq. (17) is the contribution from the integral around the saddle point at $t = t_+$ along the contour $\tilde{C}$. This term is not manifestly suppressed by $1/\sqrt{\xi}$. As far as $\alpha(\theta)$ is fixed, this term does not vanish in the limit $\xi \to \infty$. Of course, if we fix Δ and θ first, and take the limit $\xi \to \infty$, the argument of the error function goes to $+\infty$ and the function itself vanishes. However, $\alpha(\theta)$ vanishes at $\theta = \pi\Delta/(1-\Delta)$. Hence even for a very large value of ξ there is always a region of θ in which this second term cannot be neglected. However, for θ in such a region, $\alpha(\theta)$ cannot be very large. Therefore, we can safely drop the second term in the exponent. On the other hand, the last term in Eq. (17), which is the contribution from the saddle point at $t = t_-$, is always suppressed by $1/\sqrt{\xi}$. Hence, this term does not give any significant contribution for $\xi \gg 1$. The first term in Eq. (14) can be dropped in the same manner for $\xi \gg 1$. Keeping only the terms which possibly remain in the limit $\xi \to \infty$, we finally obtain

$$\begin{aligned}\phi(\xi, \theta) \approx{}& \exp\left(i\xi\cos\frac{\alpha(\theta)}{\sqrt{\xi}}\right)\Theta(\alpha(\theta)) - \frac{\sigma(\theta)}{\sqrt{\pi}}e^{i\xi - (i/2)\alpha^2(\theta)} \\ &\times \mathrm{Erfc}\left(\frac{|\alpha(\theta)|}{\sqrt{2}}e^{-i\pi/4}\right) + (\theta \to -\theta).\end{aligned} \tag{21}$$

For illustrative purpose, we compared the estimate given in Eq. (17) with the exact solution Eq. (10) in Fig. 2. They agree quite well at $\xi \gg 1$. The deficit angle and the observer's direction are chosen to be $\Delta = 0.0025$ and $\theta = 0$, respectively.

B. Geometrical optics limit

Geometrical optics limit corresponds to the limit $\xi \to \infty$ with Δ and θ fixed. In this limit $\alpha(\theta)$ also goes to $+\infty$, and hence the error function in Eq. (21) vanishes. Hence the wave form in the geometrical optics limit, which we denote as ϕ_{go}, becomes

$$\begin{aligned}\phi_{\mathrm{go}}(\xi, \theta) = {}& e^{i\xi\cos(\pi\Delta + \varphi)}\Theta(\pi\Delta + \varphi) \\ &+ e^{i\xi\cos(\pi\Delta - \varphi)}\Theta(\pi\Delta - \varphi),\end{aligned} \tag{22}$$

where φ is defined by Eq. (3).

Since ϕ and hence ϕ_{go} are even in θ, it is sufficient to consider the case with $\theta > 0$. In Fig. 3, the configuration of

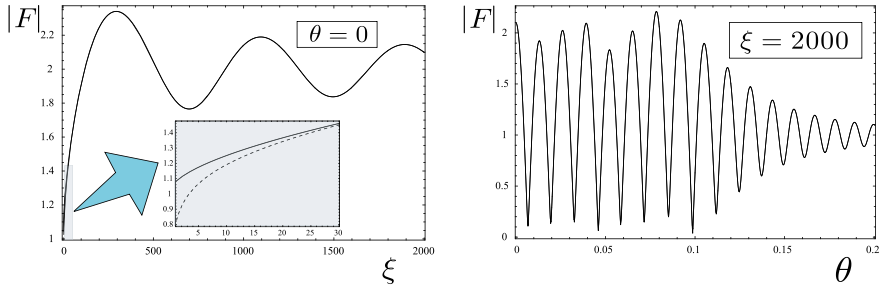

FIG. 2 (color online). Comparison between the exact solution Eq. (10) and the approximate one Eq. (17). $\pi\Delta$ is 0.0025. The black line and dotted line correspond to the exact solution and the approximate one, respectively. We see that except for small ξ the dotted line overlaps the black one. In the right panel, the relative error is about 10^{-3}.

the source, the lense, and the observer are drawn in the coordinates in which the deficit angle $2\pi\Delta$ is manifest, i.e., the wedge AOB is removed from the spacetime. Both points A and B indicate the location of the source. The lines OA and OB are to be identified. The angle made by these two lines is the deficit angle. The locations of the string and the observer are represented by O and P, respectively. In our current setup the distance between O and A ($= r_o$) is taken to be infinite. When $\varphi > \pi\Delta$, only the source A can be seen from the observer. This corresponds to the fact that only the first term remains for $\varphi > \pi\Delta$ in Eq. (22). For $\varphi > \pi\Delta$, we have

$$\phi_{\rm go}(\xi, \theta) = e^{i\xi\cos(\varphi+\pi\Delta)}. \tag{23}$$

This is a plane wave whose traveling direction is $\varphi = -\pi\Delta$, which is the direction of $\vec{\rm AP}$ in Fig. 3 in the limit $r_o = |\vec{\rm AO}| \to \infty$.

For $|\varphi| < \pi\Delta$, $\phi_{\rm go}$ is

$$\phi_{\rm go}(\xi, \theta) = e^{i\xi\cos(\varphi-\pi\Delta)} + e^{i\xi\cos(\varphi+\pi\Delta)}. \tag{24}$$

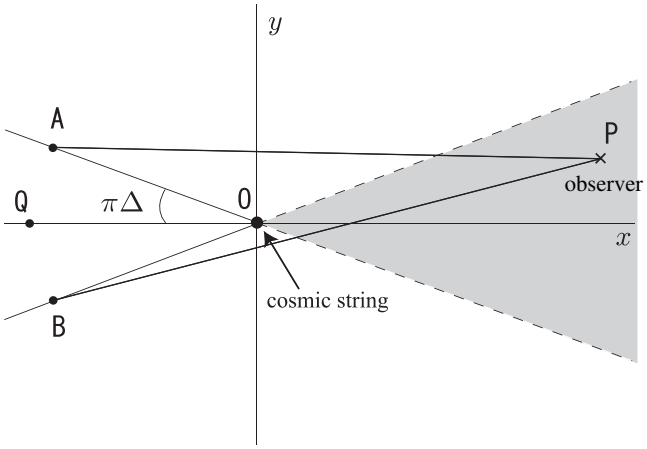

FIG. 3. Configuration of the source, the cosmic string, and the observer. A and B are the positions of a source. O and P are the positions of the cosmic string and the observer, respectively. In this figure, the wedge AOB is removed and thus A and B must be identified.

This is the superposition of two plane waves whose traveling directions are different by the deficit angle $2\pi\Delta$. Hence amplification of the images and interference occur for $|\varphi| < \pi\Delta$ as expected.

As we shall explain below, Eq. (22) coincides with the one derived under the geometrical optics. In geometrical optics, wave form is given by [11]

$$\phi_{go} = \sum_j |u(\vec{x}_j)|^{1/2} \exp[i\omega T(\vec{x}_j) - i\pi n_j], \tag{25}$$

where $\vec{x}$ represents a two-dimensional vector on the lens plane and $T(\vec{x})$ represents the summation of time of flight of the light ray from the source to the point $\vec{x}$ on the lens plane and that from the point $\vec{x}$ to the observer. $\vec{x}_j$ is a stationary point of $T(\vec{x})$, and $n_j = 0, 1/2, 1$ when $\vec{x}_j$ is a minimum, saddle, and maximum point of $T(\vec{x})$, respectively. The amplitude ratio $|u(\vec{x})|^{1/2}$ is written as

$$u(\vec{x}) = 1/\det[\delta_{ab} - \partial_a\partial_b\psi(\vec{x})], \tag{26}$$

where $\psi(\vec{x})$ in Eq. (26) is the deflection potential [47] which is the integral of the gravitational potential of the lens along the trajectory between the source and the observer. Equation (25) represents that the wave form is obtained by taking the sum of the amplitude ratio $|u(\vec{x}_j)|^{1/2}$ of each image with the phase factor $e^{i\omega T(\vec{x}_j) - i\pi n_j}$. If the lens is the straight string, the spacetime is locally flat everywhere except for right on the string. This means that the deflection potential $\psi(\vec{x})$ is zero and hence the amplitude ratio is unity for all images [47] and the trajectory where the time of flight $T(\vec{x})$ takes the extremal value is a geodesic in the conical space, and $T(\vec{x})$ of any geodesic takes minimum, which means $n_j = 0$. There are two geodesics if the observer is in the shaded region in Fig. 3. The time of flight along the trajectory AP is

$$T_{\rm A} = \lim_{r_o\to\infty} |\vec{\rm AP}| \approx r_o + r\cos(\pi\Delta + \varphi), \tag{27}$$

where $r \equiv |\vec{\rm OP}|$. The time of flight along the trajectory BP is obtained by just replacing φ with $-\varphi$. Hence, substituting (27) into (25), we find that the wave form in the geometrical optics is the same as Eq. (24) except for an

overall phase $e^{ir_o\xi}$. This factor has been already absorbed in the choice of the normalization factor B in our formula (10).

We define the amplification factor

$$F(\xi,\theta)=\frac{\phi(\xi,\theta)}{\phi_{\rm UL}(\xi,\theta)}, \tag{28}$$

where $\phi_{\rm UL}$ is the unlensed wave form. Using Eq. (24), the amplification factor of $\phi_{\rm go}$ for $|\varphi|<\pi\Delta$ is given by

$$F_{\rm go}(\xi,\theta)\approx 2e^{-i\frac{\xi}{2}(\pi\Delta)^2}\cos(\pi\Delta\xi\varphi), \tag{29}$$

where we have assumed φ and Δ are small and dropped terms higher than quadratic order. It might be more suggestive to rewrite the above formula into

$$|F_{\rm go}(\xi,\theta)|\approx 2\cos(\pi\Delta\omega y), \tag{30}$$

where $y=r\sin\varphi$. The distance from a node to the next of when the observer is moved in y-direction is $\lambda/\pi\Delta$, where λ is a wavelength. This oscillation is seen in the right panel of Fig. 2.

C. Quasigeometrical optics approximation

In the previous subsection, we have derived the wave form in the limit $\xi, |\alpha(\pm\theta)|\to\infty$ which corresponds to the geometrical optics approximation. Here we expand the wave form (21) to the lowest order in $1/\alpha(\pm\theta)$. This includes the leading order corrections to the geometrical optics approximation due to the finite wavelength effects.

For the same reason as we explained in the previous subsection, we assume that Δ and φ are small. Using the asymptotic formula for the error function Eq. (A6), the leading order correction due to the finite wavelength, which we denote as $\delta\phi_{\rm qgo}$, is obtained as

$$\begin{aligned}\delta\phi_{\rm qgo}(\xi,\theta)&=-\frac{e^{i\xi+i\pi/4}}{\sqrt{2\pi}}\left(\frac{1}{\alpha(\theta)}+\frac{1}{\alpha(-\theta)}\right)\\&=-\frac{e^{i\xi+i\pi/4}}{\sqrt{2\pi\xi}}\,\frac{2\pi\Delta}{(\pi\Delta)^2-\varphi^2}.\end{aligned} \tag{31}$$

As is expected, the correction blows up for $|\varphi|\approx\pi\Delta$, where $\alpha(\theta)$ or $\alpha(-\theta)$ vanishes, irrespective of the value of ξ. In such cases, we have to evaluate the error function directly, going back to Eq. (21).

The expression on the first line in Eq. (31) manifestly depends only on $\alpha(\pm\theta)$ aside from the common phase factor $e^{i\xi}$. This feature remains true even if we consider a small value of $\alpha(\pm\theta)$. This can be seen by rewriting Eq. (21) as

$$\phi(\xi,\theta)\approx\frac{e^{i\xi-(i/2)\alpha^2(\theta)}}{\sqrt{\pi}}\,{\rm Erfc}\left(\frac{-\alpha(\theta)}{\sqrt{2i}}\right)+(\theta\to-\theta). \tag{32}$$

The common phase $e^{i\xi}$ does not affect the absolute magnitude of the wave. Except for this unimportant overall phase, the wave form is completely determined by $\alpha(\pm\theta)$.

The geometrical meaning of these parameters $\alpha(\pm\theta)$ is the ratio of two length scales defined on the lens plane. To explain this, let us take the picture that a wave is composed of a superposition of waves which go through various points on the lens plane. In the geometrical optics limit the paths passing through stationary points of $T(\vec{x})$, which we call the image points, contribute to the wave form. The first length scale is $r_s=|\alpha(\pm\theta)|/\sqrt{\xi}\times r$ which is defined as the separation between an image point and the string on the lens plane. In this picture we expect that paths whose pathlength is longer or shorter than the value at an image point by about one wavelength will not give a significant contribution because of the phase cancellation. Namely, only the paths which pass within a certain radius from an image point need to be taken into account. Then such a radius will be given by $r_F=\sqrt{\lambda r}$, which we call Fresnel radius. Namely, a wave with a finite wavelength can be recognized as an extended beam whose transverse size is given by r_F. The ratio of these two scales gives $\alpha(\pm\theta)$:

$$|\alpha(\pm\theta)|=\frac{\sqrt{2\pi}r_s}{r_F}.$$

When $r_s\gg r_F$, i.e., $\alpha(\pm\theta)\gg 1$, the beam width is smaller than the separation. In this case the beam image is not shadowed by the string, and therefore the geometrical optics becomes a good approximation. When $r_s\lesssim r_F$, i.e.,

$$\alpha(\pm\theta)\lesssim 1, \tag{33}$$

we cannot see the whole image of the beam, truncated at the location of the string. Then the diffraction effect becomes important. The ratio of the beam image eclipsed by the string determines the phase shift and the amplification of the wave coming from each image. If we substitute $|\varphi|\approx 0$ as a typical value, we obtain a rough criterion that the diffraction effect becomes important when

$$\lambda\gtrsim 2\pi(\pi\Delta)^2 r, \tag{34}$$

or $\xi\lesssim(\pi\Delta)^{-2}$ in terms of ξ.

The same logic applies for a usual compact lens object. In this case the Fresnel radius does not change but the typical separation of the image from the lens is given by the Einstein radius $r_E\approx\sqrt{4GMr}$, where M is the mass of the lens. Then the ratio between r_E and r_F is given by $r_E/r_F=\sqrt{GM/\lambda}$, which leads to the usual criterion that the diffraction effect becomes important when $\lambda\gtrsim GM$ [1–5].

From the above formula (31), we can read that the leading order corrections scales like $\propto\sqrt{\lambda/r}$. This dependence on λ and r differs from the cases that the lens is composed of a normal localized object, in which the leading order correction due to the finite wavelength is $\mathcal{O}(\lambda/M)$ [15].

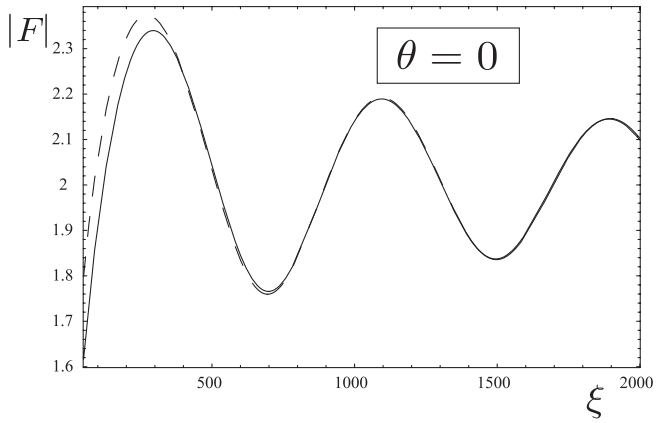

FIG. 4. The absolute value of the amplification factor as a function of ξ for $\theta = 0$. The black line and dashed line correspond to Eq. (21) and the quasigeometrical optics approximation, respectively. The string tension is chosen to be $G\mu = 10^{-2}$.

The condition for the diffraction effect to be important (33) can be also derived directly from Eq. (31). In order that the current expansion is a good approximation, $\phi_{\rm qgo}$ must be smaller than $\phi_{\rm go}$. This requires that $1/\alpha(\pm\theta) \gg 1$, which is identical to (33).

We plot the absolute value of the amplification factor under the quasigeometrical optics approximation as a dashed line in Fig. 4. We find that the quasigeometrical optics approximation is a good approximation for $\xi \gtrsim \Delta^{-2}$. For $\xi \lesssim \Delta^{-2}$, the quasigeometrical optics approximation gives a larger amplification factor than the exact one.

In the quasigeometrical optics approximation, we find from Eqs. (24) and (31) the absolute value of the amplification factor for $\varphi = 0$ is

$$|F(\xi, 0)| \approx 2\left[1 - \sqrt{\frac{2}{\pi\xi(\pi\Delta)^2}}\cos\left(\frac{\xi}{2}(\pi\Delta)^2 + \frac{\pi}{4}\right)\right]^{1/2}. \tag{35}$$

From this expression, we find that the position of the first peak of the amplification factor lies at $\xi \approx 4.25 \times (\pi\Delta)^{-2}$, which can be also verified from Fig. 4. For $\xi \lesssim \Delta^{-2}$ the present approximation is not valid, but we know that the amplification factor should converge to unity in the limit $\xi \to 0$, where r_F is much larger than r_s.

We show in Fig. 5 the absolute value of the amplification factor as a function of φ for four cases of ξ around Δ^{-2}. Top left, top right, bottom left, and bottom right panels correspond to $\xi(\pi\Delta)^2 = 0.5$, 1, 2, and 4, respectively. Black curves are plots for Eq. (21) and the dotted ones are plots for the quasigeometrical optics approximation. As is expected, the error of the quasigeometrical optics approximation becomes very large near $\varphi = \pi\Delta$, where $\alpha(\theta)$ vanishes. As the value of ξ increases, the angular region in which the quasigeometrical optics breaks down is reduced.

Interestingly, the absolute value of the amplification factor deviates from unity even for $\varphi \gtrsim \pi\Delta$ which is not observed in the geometrical optics limit. This is a consequence of diffraction of waves, the amplitude of oscillation of the interference pattern becomes smaller as θ becomes larger, which is a typical diffraction pattern formed when a wave passes through a single slit. The broadening of the interference pattern due to the diffraction effect means that the observers even in the region $|\varphi| > \pi\Delta$ can detect signatures of the presence of a cosmic string.

But the deviation of the amplification from unity outside the wedge $\varphi > \pi\Delta$ is rather small except for the special case $\xi(\pi\Delta)^2 \approx 1$: for $\xi(\pi\Delta)^2 \ll 1$ the magnification is

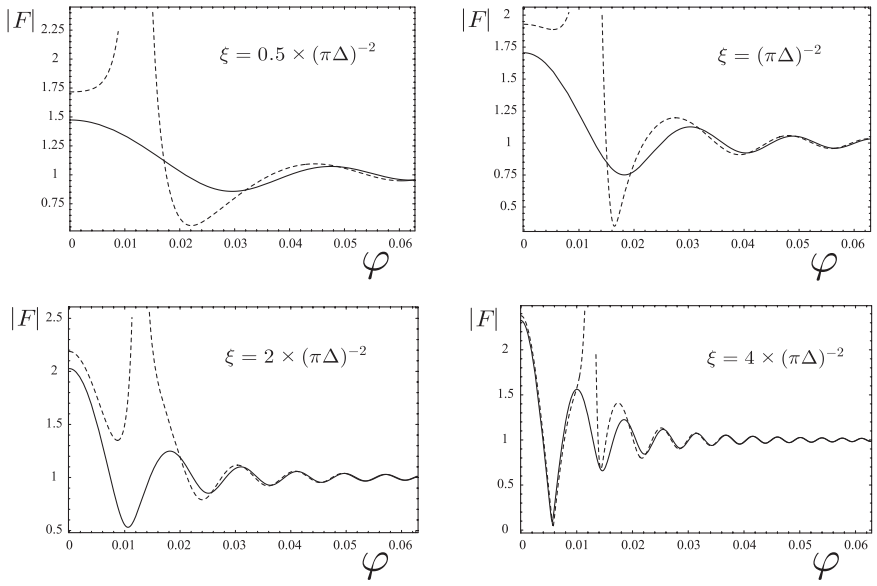

FIG. 5. The black line and dotted line correspond to Eq. (21) and the quasigeometrical optics approximation, respectively. The string tension is chosen to be $G\mu = 10^{-3}$.

inefficient and for $\xi(\pi\Delta)^2 \gg 1$ the magnification itself does not occur. Hence the increase of the event rates of lensing by cosmic strings compared with the estimate under the geometrical optics approximation could be important only when the relation $\xi(\pi\Delta)^2 \approx 1$ is satisfied. If we take $D = 10^{28}$ cm and $\omega = 10^{-3}$ Hz which is in the frequency band of laser interferometer space sntenna (LISA) [48], we find that the typical value of $G\mu$ is $\approx 2 \times 10^{-9}$.

So far, we have considered the stringy source rather than a point source. Extension to a point source can be done in a similar manner to the case of the stringy source and is treated in Appendix B. The result is

$$\phi(r, \theta, z) \approx -\frac{1}{4\pi D} e^{i\omega D} \mathcal{F}\left(\frac{\omega r r_o}{D}, \theta\right), \tag{36}$$

where $D = \sqrt{(r + r_o)^2 + z^2}$ is the distance between the source and the observer. $\mathcal{F}$, which is defined by Eq. (B14), is related to ψ as

$$\mathcal{F}(x, \theta) = [e^{-i\xi}\psi(\xi, \theta)]|_{\xi \to x} + (\theta \to -\theta). \tag{37}$$

Hence ϕ for the point source is similar to that for the stringy source. In particular, assuming that $\Delta, \varphi \ll 1$, and keeping terms which could remain for $\omega r, \omega r_o \gg 1$, we have

$$F\left(\frac{\omega r r_o}{D}, \theta\right) \approx e^{-(i/2)[(\omega r r_o)/D](\pi\Delta - \varphi)^2} \frac{1}{\sqrt{\pi}} \times \mathrm{Erfc}\left(\frac{\varphi - \pi\Delta}{\sqrt{2i}} \sqrt{\frac{\omega r r_o}{D}}\right) + (\theta \to -\theta). \tag{38}$$

D. Simpler derivation of Eq. (32).

We have derived an approximate wave form (32) which is valid in the wave zone from the exact solution of the wave equation Eq. (10). Here we show that Eq. (32) can be obtained by a more intuitive and simpler method. In the path integral formalism [11], the wave form is given by the sum of the amplitude $\exp(i\omega T(s))$ for all possible paths which connect the source and the observer. Here $T(s)$ is the time of flight along the path s. If the cosmic string resides between the source and the observer, the wave form will be given by the sum of two terms one of which is obtained by the path integral over the paths which pass through the upper side of the string ($y > 0$) in Fig. 3, and the other through the lower side of it ($y < 0$). The wave form coming from the former contribution will be given by

$$A \int_{-\infty}^{\infty} dz_{\mathrm{Q}} \int_{0}^{\infty} dy_{\mathrm{Q}} e^{i\omega(|\vec{\mathrm{AQ}}| + |\vec{\mathrm{QP}}|)}, \tag{39}$$

where $\mathrm{Q} = (0, y_{\mathrm{Q}}, z_{\mathrm{Q}})$ is a point on the lens plane specified by $x = 0$. One can determine the normalization constant A by a little more detailed analysis, but we do not pursue it further here. By integrating Eq. (39), we recover the first term in Eq. (32).

E. Long wavelength limit

For completeness, we consider the case in which the wavelength is longer than the distance from the string $\xi \lesssim 1$. In this limit, the first few terms in Eq. (10) dominate, and we find

$$\phi(\xi, \theta) \approx \frac{1}{1 - \Delta} + i \frac{e^{-\Delta \log 2 - \pi\Delta/2i}}{\Gamma(1 + \Delta)} \xi^{1+\Delta} \cos\theta. \tag{40}$$

In particular, for $\xi \to 0$ Eq. (40) becomes $(1 - \Delta)^{-1}$ which is larger than unity. This differs from the cases of gravitational lensing by a normal compact object, where the amplification becomes unity in the long wavelength limit. The reason why the amplification differs from unity even in the long wavelength limit is that the space has a deficit angle and hence the structure at the spatial infinity is different from the usual Euclidean space. Waves with very long wavelengths do not feel the local structure of string. However, uniform amplification of waves should occur as a result of total energy flux conservation because the area of the asymptotic region at a constant distance from the source is reduced due to the deficit angle. In this sense such modes feel the existence of a string.

IV. CONNECTIONS TO OBSERVATIONS

A. Compact binary as a source

In this section, we consider compact binaries as sources of gravitational waves. Gravitational waves from compact binaries are clean in the sense that the waves are almost monochromatic: the time scale for the frequency to change is much longer than the orbital period of the binary except for the phase just before plunge. Hence interference between two waves coming from both sides of the cosmic string could be observed by future detectors.

Since each compact binary has a finite lifetime, lensing events can be classified roughly into two cases. If the difference between the times of flight along two geodesics is larger than the lifetime of the binary, we will observe two independent waves separately at different times. On the other hand, if the time delay is shorter than the lifetime, what we observe is the superposition of two waves.

The remaining lifetime of the binary T_{life} when the period of the gravitational waves measured by an observer is P_{GW} is estimated as

$$T_{\mathrm{life}} \approx 9.2 \times 10^{-4} \frac{1}{(1 + z_S)^{5/3}} \frac{(1 + \eta)^{1/3}}{\eta} \left(\frac{P_{GW}}{GM}\right)^{5/3} P_{GW}, \tag{41}$$

where η is the mass ratio of the binary ($\eta \leq 1$), M is the mass of the more massive star in the binary, and z_S is the source redshift.

The time delay T_{delay} is

$$T_{\mathrm{delay}} \approx 2 \frac{r r_o}{D} \varphi \pi\Delta. \tag{42}$$

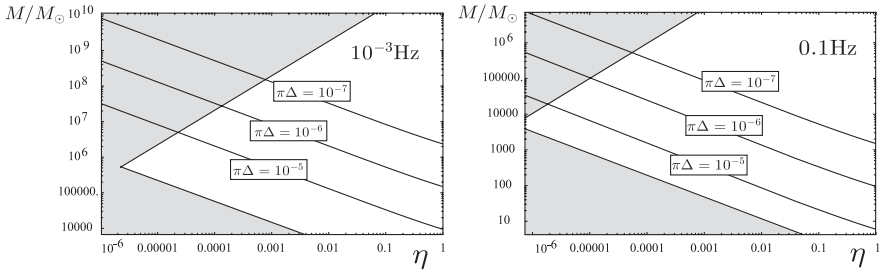

FIG. 6. Plots of regions where Eq. (43) is satisfied for three different values of the string parameter. Left and right panels are for 10^{-3} Hz and 0.1 Hz which are the frequency bands LISA and DECIGO have best sensitivities. Shaded regions are plotted under the assumptions that the signals satisfy $SN > 10$, the redshift of the source is 1 and 3 yr observations.

Taking the typical values of parameters as $rr_o/D = 1$ Gpc and $\varphi = \pi\Delta$, the condition $T_{\rm life} \gg T_{\rm delay}$ gives the upper bound on the mass M,

$$M \ll 8 \times 10^3 \frac{(1+\eta)^{1/5}}{\eta^{3/5}} \left(\frac{\pi\Delta}{10^{-5}}\right)^{-6/5} \left(\frac{P_{GW}}{10^3 \ \sec}\right)^{8/5} M_\odot. \tag{43}$$

The time scale for the orbital frequency of the binary to change is the same order as $T_{\rm life}$. Hence the condition $T_{\rm life} \gg T_{\rm delay}$ implies that the frequencies of two waves are almost the same. The left and right panels in Fig. 6 which correspond to different frequencies of gravitational waves show the region where the condition Eq. (43) is satisfied for three different values of string parameter Δ. The shaded area represents the parameter region beyond the detector's sensitivities. In the left and right panels we assumed, respectively, that the threshold value for detection in strain amplitude for LISA and DECIGO [49]/BBO [50], which are given by 10^{-20} Hz$^{-1/2}$ and 10^{-23} Hz$^{-1/2}$. We find that both cases $T_{\rm life} \gg T_{\rm delay}$ and $T_{\rm life} \ll T_{\rm delay}$ can occur both for LISA and BBO/DECIGO.

B. Wave form

We can easily extend our wave form (10) to the case that the frequency of the source changes in time. Let us write the source as $\frac{1}{1-\Delta} S(t)\delta(r - r_o)\delta(\theta - \pi)\delta(z)$. The Fourier transformation of $S(t)$ is defined by

$$S(t) = \int_{-\infty}^{\infty} d\omega \ e^{-i\omega t} S_\omega. \tag{44}$$

Denoting the solution $\phi(t, \vec{x})$ for a monochromatic source obtained in the previous sections by $\phi_\omega(\vec{x})$, ϕ can be written as

$$\phi(t, \vec{x}) = \int_0^{\infty} d\omega \, e^{-i\omega t} S_\omega \phi_\omega(\vec{x}) + \text{c.c.}, \tag{45}$$

where we assumed that $S(t)$ is real. Substituting Eq. (36) to the above expression, we have

$$\phi(t, \vec{x}) \approx -\frac{1}{4\pi D} \int_0^{\infty} d\omega \, e^{-i\omega(t-D)} \mathcal{F}\left(\frac{\omega r r_o}{D}, \theta\right) S_\omega + \text{c.c.} \tag{46}$$

Equation (46) is a general formula which applies to any time dependent source. Here we consider the special case in which $S(t)$ takes the form

$$S(t) = \cos\left(\int_0^t dt' \Omega(t')\right), \tag{47}$$

with

$$\Omega(t) = \omega_o + \dot{\omega}_o t, \tag{48}$$

where $\dot{\omega}_o/\omega_o^2 \ll 1$ and $\omega_o > 0$ are assumed. This represents a quasimonochromatic source with its frequency slowly changing. Then S_ω is

$$S_\omega = \frac{1}{\sqrt{2\pi\dot{\omega}_o}} (e^{-i[(\omega+\omega_o)^2/(2\dot{\omega}_o)]+i\pi/4} + e^{i[(\omega-\omega_o)^2/(2\dot{\omega}_o)]-i\pi/4}). \tag{49}$$

Substituting Eqs. (38) and (49) into Eq. (46), and using the method of the steepest descent, we have

$$\phi(t, \vec{x}) \approx \frac{1}{4\pi\sqrt{\pi}D} \text{Erfc}\left(\frac{\varphi - \pi\Delta}{\sqrt{2i}} \sqrt{\frac{\Omega(T(\varphi)) r r_o}{D}}\right) \times e^{-iT(\varphi)(\omega_o + (1/2)\dot{\omega}_o T(\varphi))} + \text{c.c.} + (\varphi \to -\varphi), \tag{50}$$

with

$$T(\varphi) = t - D + \frac{r r_o}{2D}(\pi\Delta - \varphi)^2. \tag{51}$$

This represents a superposition of two waves coming from both sides of the string whose arrival times differ by $|T(\varphi) - T(-\varphi)| = [(2rr_o)/D]\pi\Delta|\varphi|$. In the preceding subsections, we study the wave forms observed in two cases with $T_{\rm life} \gg T_{\rm delay}$ and $T_{\rm life} \ll T_{\rm delay}$.

1. $T_{\rm life} \gg T_{\rm delay}$

As we have explained in the preceding subsection, what we observe is a superposition of two waves in this case. Because the relative phase difference of these waves slowly increases or decreases in time due to the frequency change of the binary source and the optical path difference between two geodesics, we will observe the beat if the amplitude of the integrated relative phase difference over observation time is larger than $\mathcal{O}(1)$.

The condition that the beat is observed can be derived as follows. If we denote the total observation period by $T_{\rm obs}$, then from Eq. (50) the integrated relative phase difference is $2\pi\Delta\varphi D\dot{\omega}_o T_{\rm obs}$, where both r and r_o are assumed to be $O(D)$. Hence we can observe the beat if

$$T_{\rm obs} \gtrsim \frac{1}{2\pi\Delta\varphi D\dot{\omega}_o}. \tag{52}$$

Because $T_{\rm life}$ is roughly the same as the time scale for the frequency of the binary to change, i.e. $T_{\rm life} \sim \omega_o/\dot{\omega}_o$, Eq. (52) can be written as

$$T_{\rm obs} \gtrsim \frac{T_{\rm life}}{2\pi\Delta\varphi D\omega_o}. \tag{53}$$

If $T_{\rm obs}$ is fixed, e.g. $T_{\rm obs} \sim 3$ yr for LISA, Eq. (53) is written as an lower bound on M. For $T_{\rm obs} = 3$ yr and $P_{GW} = 10^3$ sec, Eq. (53) becomes

$$M \gtrsim 2.6 \times \frac{(1+\eta)^{1/5}}{\eta^{3/5}} \left(\frac{\pi\Delta}{10^{-5}}\right)^{-6/5} \left(\frac{P_{GW}}{10^3\ \text{sec}}\right)^{13/5} M_\odot. \tag{54}$$

We show in Fig. 7 the region where Eq. (54) is satisfied for LISA with $T_{\rm obs} = 3$ yr. We find that if $G\mu \lesssim 2.8 \times 10^{-8}$ which is about 1 order of magnitude below the current upper bound, LISA will detect the beat of gravitational waves for all observable ranges in (μ, M) space as long as $T_{\rm life} \gg T_{\rm dely}$.[2]

2. $T_{\rm life} \ll T_{\rm delay}$

If $T_{\rm delay} \gg T_{\rm life}$, we observe the wave form of either the first term or the second one in Eq. (50) at a given time. We show in Fig. 8 the amplification of the wave corresponding to the first term in Eq. (50) as a function of $\varphi - \Delta\pi$ normalized by $1/\sqrt{\omega r r_o/D}$, which is nothing but $-\alpha(\theta)$ in the case discussed in Sec. III. We find that the amplification approaches zero more slowly for $\varphi - \pi\Delta > 0$ and oscillates around unity for $\varphi - \pi\Delta < 0$ and the angular size in which nontrivial oscillations due to the diffraction effect can be observed is given by $1/\sqrt{\omega r r_o/D}$. Since $T_{\rm delay} \approx (r r_o/D)\varphi\pi\Delta < T_{\rm life} \ll \omega^{-1}$ in the present case, we have $(r r_o/D)(\pi\Delta)^2 \gtrsim (r r_o/D)\pi\Delta\varphi \gg 1$. Therefore this angular size of oscillation is much smaller than $\pi\Delta$. Hence it will be very difficult to detect a lensing event in which this diffraction effect is relevant.

[2]Since the lensing probability is not expected to be high, we need a large number of events to detect a lensing event. In such a situation, what gravitational wave detectors can detect is a superposition of various waves. Hence, signal will almost always have beat even if we ignore the lensing effect.

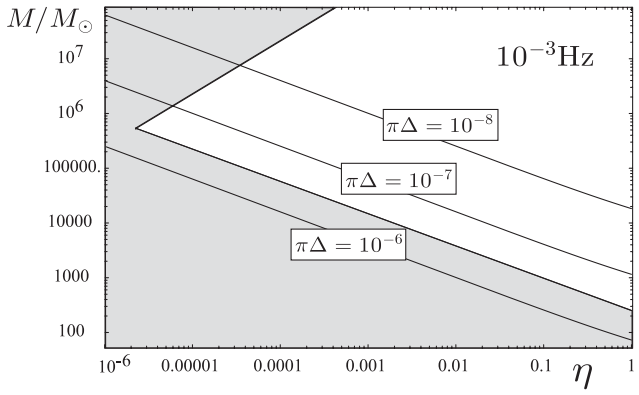

FIG. 7. Plot of the region where Eq. (54) is satisfied. The frequency of the gravitational waves is assumed to be 10^{-3} Hz.

C. Estimation of the event rate

In this section, we estimate the detection rate of the gravitational lensing caused by cosmic strings for planned gravitational wave detectors such as LISA, DECIGO, and BBO.

It is well known that string network obeys the scaling solution where the appearance of the string network at any time looks alike if it is scaled by the horizon size. There are a few dozen strings spread crossing the horizon volume and a number of string loops [51–53]. Since the horizon scale increases in the comoving coordinates as time goes, the number of strings increase if there is no interaction between them. However, since strings are typically moving at a relativistic speed, they frequently intersect with each other. As a result reconnection between strings occurs, reducing the number of long strings which extend over the horizon scale. During the process of reduction of the number of long strings a large number of string loops are formed, but they shrink and decay via gravitational radiation. Due to the balance of two effects, the number of long strings in a horizon volume remains almost constant in time.

The reconnection probability p is essentially 1 for gauge theory solitons [54] because reconnection allows the flux inside the string to take an energetically favorable shortcut. For F-strings, the reconnection is a quantum process and its probability is roughly estimated as $p \sim g_s^2$, where g_s is the string coupling and is predicted in [55] that

$$10^{-3} \lesssim p \lesssim 1. \tag{55}$$

For D-strings, the reconnection probability might be $0.1 \lesssim p \lesssim 1$ [55]. If the reconnection probability is less than 1, the number of long strings is expected to be p^{-1} times larger than that in the case with $p = 1$. Therefore it is

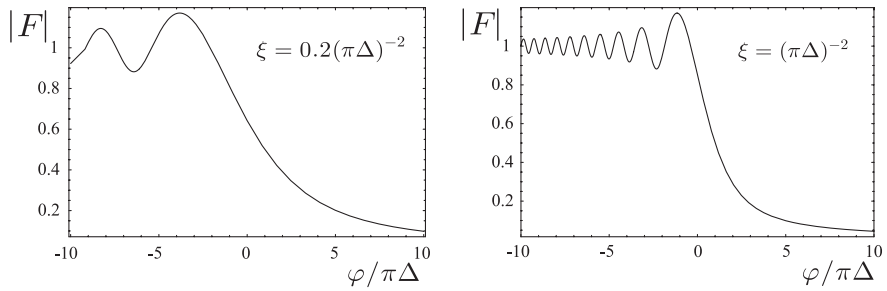

FIG. 8. The absolute value of the amplification factor for $T_{\rm life} \ll T_{\rm delay}$ as a function of φ. Left and right panels correspond to $\xi = 0.2(\pi\Delta)^{-2}$ and $(\pi\Delta)^{-2}$, respectively.

expected that in the context of cosmic strings motivated by superstring theory the number of long strings in a horizon volume can be 10^3 or more.

To estimate the event rate for the gravitational lensing, here we consider a compact binary (such as binary neutron stars and/or black holes) as a source of gravitational waves. There are large uncertainties about the event rate of massive black hole (MBH) merger detected by LISA or DECIGO/BBO. Several authors [56–58] employed a model in which MBH mergers are associated with the mergers of host dark matter halos to estimate the event rate of MBH-MBH mergers. In this model, the event rate is dominated by halos with the minimum mass $M_{\rm min}$ above which halos have a central MBH and some scenarios predict that the event rate could reach $\sim 10^4$ events/yr. For DECIGO/BBO, the binary neutron stars will be observed $\sim 10^5$ events/yr.

The probability of lensing for a single source by an infinite straight cosmic string both at cosmological distances is

$$P \simeq 3 \times 10^{-6}\left(\frac{\pi\Delta}{10^{-5}}\right). \tag{56}$$

Equation (56) is derived under the geometrical optics approximation. In Section III, we found that the signal of lensing by cosmic strings (the interference pattern of gravitational waves at detectors) extends over angular scales larger than the deficit angle $2\pi\Delta$ when the diffraction effect is marginally important. This is a well-known fact for the gravitational lensing by usual stellar objects [6,59]. As we estimated in Section III, the critical distance D_c below which the diffraction effect becomes important is

$$D_c = 50\left(\frac{P_{GW}}{10^3\ \text{sec}}\right)\left(\frac{\pi\Delta}{10^{-5}}\right)^{-2}\ \text{kpc}. \tag{57}$$

Therefore the probability of lensing by cosmic strings may be enhanced due to the diffraction effect for $\pi\Delta \approx 10^{-7}$ at LISA band ($P_{GW} \approx 10^3$ sec) and for $\pi\Delta \approx 10^{-8}$ at DECIGO/BBO band ($P_{GW} \approx 10$ sec).

Assuming the prospective values of the parameters that determines the rate of lensing events $\dot{n}$, we obtain

$$\dot{n} \sim 3f\left(\frac{p}{0.1}\right)^{-1}\left(\frac{\pi\Delta}{10^{-5}}\right)\left(\frac{\dot{n}_S}{10^5\ \text{yr}^{-1}}\right)\ \text{yr}^{-1}, \tag{58}$$

where $f(>1)$ denotes the numerical factor arising from the enhancement of the lensing probability due to the diffraction effect. $\dot{n}_S = 10^5$ is almost upper bound on the total event rate of neutron star mergers detectable by DECIGO/BBO. If the event rate is even higher, the number of events becomes comparable to or larger than the number of frequency bins. Then we will not be able to distinguish each event, and undistinguishable signals become confusion noise. In the case of LISA, this bound on $\dot{n}_S$ is even lower. Unfortunately, a large number of lensing events by cosmic strings can be expected only for marginally large $\pi\Delta(\approx G\mu/4)$ with a small reconnection probability p.

Finally we briefly comment on the validity of the assumption that most cosmic strings can be treated as straight ones in studying gravitational lensing by them. In geometrical optics approximation, only light paths which satisfy the Fermat's principle contribute to the amplification factor. If we take into account the finiteness of the wavelength, the trajectories whose optical path differences are less than a few times of its wavelength will dominantly contribute to the amplification factor. In terms of the distance on the lens plane ($x = 0$-plane in Fig. 3), the optical paths within $\lesssim \sqrt{\lambda D}$ from the intersection of the geodesic will give a dominant part of the amplification factor.

In the standard literature, the typical size of small-scale structure of a long string is given by the gravitational backreaction scale $\sim 50G\mu t$, where t is a cosmic time [60]. But this is not an established argument and some recent studies suggest that the smallest size of the wiggles could be much smaller than $50G\mu t$ [61,62]. If we assume here that the smallest size of the wiggles is $50G\mu t$, then the condition that the straight string approximation is good is $\sqrt{\lambda D} \lesssim 50G\mu t$. Substituting the appropriate values of the parameters, it gives the condition,

$$1 \gtrsim \frac{\sqrt{\lambda D}}{50G\mu t} = 8 \times 10^{-5}\left(\frac{\pi\Delta}{10^{-5}}\right)^{-1}\left(\frac{\lambda}{10^{13}\ \text{cm}}\right)^{1/2}\left(\frac{D}{10^{26}\ \text{cm}}\right)^{1/2}. \tag{59}$$

Hence approximating a cosmic string by a straight one is good for a wide range of possible values of the parameters.

V. SUMMARY

We have constructed a solution of the Klein-Gordon equation for a massless scalar field in the flat spacetime with a deficit angle $2\pi\Delta \approx 8\pi G\mu$ caused by an infinite straight cosmic string. We showed analytically that the solution in the short wavelength limit reduces to the geometrical optics limit. We have also derived the correction to the amplification factor obtained in the geometrical optics approximation due to the finite wavelength effect and the expression in the long wavelength limit.

The wave form is characterized by a ratio of two different length scales. One length scale r_s is defined as the separation between the image position on the lens plane in the geometrical optics and the string. We have two r_s since there are two images corresponding to which side of the string the ray travels. (When the image cannot be seen directly, we assign a negative number to r_s.) The other length scale r_F, which is called Fresnel radius, is the geometrical mean of the wavelength and the typical separation among the source, the lens, and the observer. The wave form is characterized by the ratios between r_s and r_F. If $r_F > r_s$, the diffraction effect becomes important and the interference patterns are formed. Even when the image in the geometrical optics is not directly seen by the observer, the interference patterns remain. In contrast, in the geometrical optics magnification and interference occur only when the observer can see two images which travel both sides of the string. Namely, the angular range where lensing signals exist is broadened by the diffraction effect. This broadening may increase the lensing probability by an order of magnitude compared with that estimated by using the geometrical optics when the distance to the source is around the critical distance D_c given in Eq. (57).

We finally estimated the rate of lensing events which can be detected by LISA and DECIGO/BBO assuming BH-BH or NS-NS mergers as a source of gravitational waves. For possible values of the parameters that determines the event rate such as string reconnection rate, string tension, and the event rate of the unlensed mergers, the lensing event rate could reach several per year.

ACKNOWLEDGMENTS

T. S. thanks Kunihito Ioka, Takashi Nakamura, and Hiroyuki Tashiro for useful comments. This work is supported in part by Grant-in-Aid for Scientific Research, No. 14047212 and No. 16740141, and by that for the 21st Century COE "Center for Diversity and Universality in Physics" at Kyoto university, both from the Ministry of Education, Culture, Sports, Science, and Technology of Japan.

APPENDIX A: DERIVATION OF EQ. (21)

Here we derive a formula Eq. (21) from the integral representation of the solution Eqs. (14) and (15). As we explained in the Sec. III, we have to calculate the integral for $\alpha(\theta) > 0$ and $\alpha(\theta) < 0$ separately.

1. $\alpha(\theta) < 0$

In this case, there are no contributions from the pole t_*. Since $\xi \gg 1$, the integral

$$\psi(\xi,\theta) = \frac{1}{1-\Delta}\frac{1}{2i\pi} \times \int_C dt \frac{e^{\xi\sinh t}}{1 - e^{-1/(1-\Delta)(t - i(\pi/2) + i\alpha(\theta)/\sqrt{\xi+\epsilon})}}, \tag{A1}$$

is dominated from the two regions $|t \pm i\frac{\pi}{2}| \lesssim 1/\sqrt{\xi}$, where $\pm i\frac{\pi}{2}$ is the saddle points of $e^{\xi\sinh t}$.

Let us first calculate the integral around $i\pi/2$. We cannot apply the method of steepest descent where the denominator of the integrated function is replaced with the value at $t = i\pi/2$ because the pole t_* of the integrand can lie in the region $|t_* - i\pi/2| \lesssim 1/\sqrt{\xi}$ and the denominator is no longer constant around $i\pi/2$.

Fortunately the integral can be approximated written by the special function which can be evaluated easily. We first do the transformation of variable such that $t - i\pi/2 = e^{i\pi/4}u$ (u:real number) which corresponds to the deformation of the contour of the integral from C to $\tilde{C}$ as shown in Fig. 1. Expanding $e^{\xi\sinh t}$ around $i\pi/2$ to second order in u and the denominator of the integral to the first order in u gives the integral

$$\frac{1}{2i\pi}\exp\left(i\xi + \frac{i\alpha(\theta)}{(1-\Delta)\sqrt{\xi}}\right)\int_{-\infty}^{\infty} du \frac{e^{-(u^2/2)}}{u + e^{i\pi/4}\tilde{\alpha}(\theta)}, \tag{A2}$$

where $\tilde{\alpha}(\theta)$ is defined by Eq. (18). Hence we need to evaluate the integral

$$I(x) := \int_{-\infty}^{\infty} du \frac{e^{-(u^2/2)}}{u - x} = \int_{\infty}^{\infty} du \frac{e^{-[(u+x)^2/2]}}{u - i\epsilon}, \tag{A3}$$

where ϵ was introduced to remember that the imaginary part of $x = -e^{i\pi/4}\tilde{\alpha}(\theta)$ is positive when $\tilde{\alpha}(\theta) < 0$. This integral is given by an error function as

$$I(x) = 2i\sqrt{\pi}e^{-x^2/2}\mathrm{Erfc}\left(-i\frac{x}{2}\right) \equiv 2i\sqrt{\pi}e^{-x^2/2}\int_{-i\frac{x}{2}}^{\infty} dt e^{-t^2}. \tag{A4}$$

This can be derived by solving a differential equation

$$\frac{d}{dx}I(x) = -\sqrt{2\pi} - xI(x), \tag{A5}$$

which follows from the definition of $I(x)$, with the boundary condition that $I(0) = i\pi$.

Asymptotic formulas for the error function are

$$\begin{aligned}\mathrm{Erfc}(z) &= e^{-z^2}\left(\frac{1}{2z} - \frac{1}{4z^3} + \cdots\right),\\ &\left(\text{for } -\frac{\pi}{4} < \arg z < \frac{\pi}{4} \quad \text{and} \quad |z| \to \infty\right),\\ &= \sqrt{\pi} + e^{-z^2}\left(\frac{1}{2z} - \frac{1}{4z^3} + \cdots\right),\\ &\left(\text{for} \quad \frac{3\pi}{4} < \arg z < \frac{5\pi}{4} \quad \text{and} \quad |z| \to \infty\right),\\ &= \sqrt{\pi} + \frac{\sqrt{\pi}}{2} - z + \frac{1}{3}z^3 + \cdots, \quad (\text{for} \quad |z| \ll 1).\end{aligned} \tag{A6}$$

Using Eq. (A3), the integral Eq. (A2) becomes

$$\frac{1}{\sqrt{\pi}} \exp\left(i\xi + \frac{i\alpha(\theta)}{(1-\Delta)\sqrt{\xi}} - \frac{i}{2}\tilde{\alpha}^2(\theta)\right)\mathrm{Erfc}\left(\frac{\tilde{\alpha}(\theta)}{\sqrt{2}}e^{3i\pi/4}\right). \tag{A7}$$

Next let us calculate the integral Eq. (A1) around $-i\pi/2$. Since the pole t_* is far from $-i\pi/2$, we can approximate the denominator of the integrated function as a constant and apply the usual saddle point method. This gives

$$\frac{1}{\sqrt{2\pi\xi}} \frac{1}{1-\Delta} \frac{e^{-i\xi + i\pi/4}}{1 - e^{[i/(1-\Delta)](\pi - \alpha(\theta)/\sqrt{\xi})}}. \tag{A8}$$

The sum of Eqs. (A7) and (A8) gives $\psi(\xi, \theta)$ for $\alpha(\theta) < 0$.

2. $\alpha(\theta) > 0$

In this case, there is a contribution from the pole t_*. Hence the integral is divided into the integral around the pole and the one whose circuit of integration is $\tilde{C}$.

The integral around the pole gives

$$\exp\left(i\xi \cos\frac{\alpha(\theta)}{\sqrt{\xi}}\right). \tag{A9}$$

The integral around $i\pi/2$ along the trajectory $\tilde{C}$ is the same as for $\alpha(\theta) < 0$ and is given by Eq. (A2). The only difference is the signature of $\tilde{\alpha}(\theta)$. By changing the integration variable from u to $-u$, $\tilde{\alpha}(\theta)$ is replaced with $-\tilde{\alpha}(\theta)$ and the overall signature flips. As a result we find that the integration along $\tilde{C}$ gives

$$-\frac{1}{\sqrt{\pi}}\exp\left(i\xi + \frac{i\alpha(\theta)}{(1-\Delta)\sqrt{\xi}} - \frac{i}{2}\tilde{\alpha}^2(\theta)\right)\mathrm{Erfc}\left(-\frac{\tilde{\alpha}(\theta)}{\sqrt{2}}e^{3i\pi/4}\right). \tag{A10}$$

Integral Eq. (A1) around $-i\pi/2$ is also given by Eq. (A8).

Combining the results of subsections A1 and A2, adding the similar terms $\psi(\xi, -\theta)$, and also using the asymptotic form of $J_0(\xi)$, we have Eq. (21).

APPENDIX B: SOURCE AT A FINITE DISTANCE

Here we consider a point source at a finite distance. For a point source,

$$S = \frac{1}{(1 - 4G\mu)r_o}\delta(r - r_o)\delta(\theta - \pi)\delta(z)e^{-i\omega t}, \tag{B1}$$

where $(1 - 4G\mu)r_o = \sqrt{-g}$. We consider a solution written in the form of the following expansion,

$$\phi(r, \theta, z) = \sum_{m=0}^{\infty}\int_{-\infty}^{\infty} dk\, f_{m,k}(r)\cos m\theta e^{ikz}. \tag{B2}$$

The solution for $f_{k,m}(r)$ is the same as $f_m(r)$ in (7) but ω contained in ξ and ξ_o are here replaced with $\sqrt{\omega^2 - k^2}$, and

$$N_m = \frac{1}{1-\Delta}\frac{\epsilon_m(-1)^m}{8i\pi}. \tag{B3}$$

First we compute $\phi_k(r, \theta) := \sum_m^{\infty} f_{m,k}(r)\cos m\theta$ for $r < r_o$. As in the case of Bessel function, we also use the integral representation for Hankel function

$$H_\nu^{(1)}(z) = \frac{1}{i\pi}\int_{C_H} ds e^{z\sinh s - \nu s}. \tag{B4}$$

Here the integration is to be performed along the path C_H presented in Fig. 1. Using the above formula and (12), we have

$$\begin{aligned}\phi_k(r, \theta) &= \sum_m^{\infty}\frac{i\epsilon_m(-1)^m}{32\pi^3(1-\Delta)}\int_{\infty - i\pi}^{\infty + i\pi} dt\, e^{\xi\sinh t - \nu_m t}\\ &\quad\times\int_{-\infty}^{\infty + i\pi} ds\, e^{\xi_o \sinh s - \nu_m s}(e^{im\theta} + e^{-im\theta})\\ &\approx \frac{i}{16\pi^3(1-\Delta)}\int_{\infty - i\pi}^{\infty + i\pi} dt\, e^{\xi\sinh t}\int_{-\infty}^{\infty + i\pi} ds\\ &\quad\times e^{\xi_o \sinh s}\left(\frac{1}{1 + e^{-[(t+s)/(1-\Delta)] + i\theta - \epsilon}}\right.\\ &\quad\left. + (\theta \to -\theta)\right).\end{aligned} \tag{B5}$$

We introduce a new variable $t' \equiv t + s - i\pi/2$. Under the assumption that $\xi_o \gg 1$, the integration over s is dominated by the contribution around $s = i\pi/2$. Hence, the integration contour for t is unaltered even if we change the integration variable from t to t'. After this change of the variable, we have

$$\begin{aligned}\phi_k(r, \theta) &\approx \frac{i}{16\pi^3(1-\Delta)}\int_{\infty - i\pi}^{\infty + i\pi} dt'\int_{-\infty}^{\infty + i\pi} ds\\ &\quad\times e^{f(t', s)}\left[\frac{1}{1 + e^{-\frac{1}{1-\Delta}(t' + i\pi/2) + i\theta - \epsilon}} + (\theta \to -\theta)\right],\end{aligned} \tag{B6}$$

where

$$f(t', s) := \xi\sinh(t' - s + i\pi/2) + \xi_o \sinh s. \tag{B7}$$

We expand the exponent around a zero of its derivative. The derivative vanishes at $s = s_0$, and s_0 is given by

$$\tanh s_0 = \frac{\xi \cosh(t' + i\pi/2) - \xi_o}{\xi \sinh(t' + i\pi/2)}. \tag{B8}$$

Taylor expansion of $f(t', s)$ around $s = s_0$ becomes

$$f(t', s) = i\sqrt{\xi^2 + \xi_o^2 - 2\xi\xi_o \cosh(t' + i\pi/2)} \times (1 + \tfrac{1}{2}(s - s_0)^2 + \cdots). \tag{B9}$$

We truncate this expansion at the quadratic order because the higher order terms are suppressed by $1/\xi$ or $1/\xi_o$. Performing Gaussian integral, we obtain

$$\phi_k(r, \theta) \approx \frac{\sqrt{2\pi}i}{16\pi^3(1 - \Delta)} \int_{\infty - i\pi}^{\infty + i\pi} dt' \frac{e^{f(t', s_0)}}{\sqrt{-f(t', s_0)}} \times \left(\frac{1}{1 + e^{-1/(1-\Delta)(t' + i\pi/2) + i\theta - \epsilon}} + (\theta \to -\theta) \right). \tag{B10}$$

Further, we expand $f(t', s_0)$ around an approximate stational point at $t' = i\pi/2$. Then we have

$$f(t', s_0) = i(\xi + \xi_o) + \frac{i\xi\xi_o}{2(\xi + \xi_o)} \left(t' - i\frac{\pi}{2} \right)^2 + \cdots. \tag{B11}$$

Again we truncate this expansion at the quadratic order for the same reason as before. Then one finds that $\phi_k(r, \theta)$ is approximately given by

$$\phi_k(r, \theta) \approx -\frac{\sqrt{2\pi}e^{i\pi/4}}{8\pi^2\sqrt{\xi + \xi_o}} \tilde{\phi}_k(r, \theta), \tag{B12}$$

where

$$\tilde{\phi}_k(r, \theta) = e^{i(\xi + \xi_o)} \mathcal{F}\left(\frac{\xi\xi_o}{\xi + \xi_o}, \theta \right), \tag{B13}$$

and

$$\mathcal{F}(x, \theta) := \frac{1}{2i\pi(1 - \Delta)} \int_{\infty - i\pi}^{\infty + i\pi} dt' e^{(ix/2)[t' - i(\pi/2)^2]} \times \left(\frac{1}{1 - e^{-\frac{1}{1-\Delta}(t' + i\pi/2) + i\theta - \epsilon}} + (\theta \to -\theta) \right). \tag{B14}$$

The function $\tilde{\phi}(r, \theta)$ is almost identical to $\phi(r, \theta)$ discussed in Sec. III, except that $e^{i\xi}$ and other ξ are replaced with $e^{i(\xi + \xi_o)}$ and $\frac{\xi\xi_o}{\xi + \xi_o}$, respectively.

Finally, we perform the integration over k. From (B14), we have

$$\phi(r, \theta, z) \approx -\frac{\sqrt{2\pi}e^{i\pi/4}}{8\pi^2} \int dk \frac{e^{i(\xi + \xi_o)}}{\sqrt{\xi + \xi_o}} e^{ikz} \mathcal{F}\left(\frac{\xi\xi_o}{\xi + \xi_o}, \theta \right). \tag{B15}$$

Since $\xi + \xi_o = \sqrt{\omega^2 - k^2}(r + r_o)$, we can invoke the saddle point method again to perform k-integral when $r + r_o$ is large. Evaluating the contribution from the saddle point at $k = \omega z/D$ with $D \equiv \sqrt{z^2 + (r + r_o)^2}$, we obtain

$$\phi(r, \theta, z) \approx -\frac{1}{4\pi D} e^{i\omega D} \mathcal{F}\left(\frac{\omega r r_o}{D}, \theta \right). \tag{B16}$$

The calculation for $r > r_o$ can be done in a completely parallel way, and the final result becomes identical to the case with $r < r_o$.

[1] H. C. Ohanian, Phys. Rev. D **8**, 2734 (1973); H. C. Ohanian, Int. J. Theor. Phys. **9**, 425 (1974); H. C. Ohanian, Astrophys. J. **271**, 551 (1983).
[2] P. V. Bliokh and A. A. Minakov, Astrophys. Space Sci. **34**, L7 (1975).
[3] R. J. Bontz and M. P. Haugan, Astrophys. Space Sci. **78**, 199 (1981)
[4] K. S. Thorne, in *Gravitational Radiation*, edited by N. Deruell and T. Piran (North-Holland, Amsterdam, 1983), p. 28.
[5] S. Deguchi and W. D. Watson, Astrophys. J. **307**, 30 (1986).
[6] R. Takahashi and T. Nakamura, Astrophys. J. **595**, 1039 (2003).
[7] N. Seto, Phys. Rev. D **69**, 022002 (2004).
[8] T. T. Nakamura, Phys. Rev. Lett. **80**, 1138 (1998).
[9] K. Yamamoto, astro-ph/0309696.
[10] C. Baraldo, A. Hosoya, and T. T. Nakamura, Phys. Rev. D **59**, 083001 (1999).
[11] T. T. Nakamura and S. Deguchi, Prog. Theor. Phys. Suppl. **133**, 137 (1999).
[12] K. Yamamoto and K. Tsunoda, Phys. Rev. D **68**, 041302(R) (2003).
[13] T. Suyama, R. Takahashi, and S. Michikoshi, Phys. Rev. D **72**, 043001 (2005).
[14] R. Takahashi, T. Suyama, and S. Michikoshi, Astron. Astrophys. **438**, L5 (2005).
[15] R. Takahashi, Astron. Astrophys. **423**, 787 (2004).
[16] M. B. Hindmarsh and T. W. B. Kibble, Rep. Prog. Phys. **58**, 477 (1995).
[17] A. Vilenkin and E. P. S. Shellard, *Cosmic Strings and Other Topological Defects* (Cambridge University Press, Cambridge, England, 2000).
[18] G. R. Dvali and S. H. H. Tye, Phys. Lett. B **450**, 72 (1999).
[19] G. R. Dvali, Phys. Lett. B **459**, 489 (1999).
[20] C. P. Burgess, M. Majumdar, D. Nolte, F. Quevedo, G. Rajesh, and R. J. Zhang, J. High Energy Phys. 07 (2001) 047.

[21] S. H. S. Alexander, Phys. Rev. D **65**, 023507 (2002).
[22] G. R. Dvali, Q. Shafi, and S. Solganik, hep-th/0105203.
[23] N. Jones, H. Stoica, and S. H. H. Tye, J. High Energy Phys. 07 (2002) 051.
[24] G. Shiu and S. H. H. Tye, Phys. Lett. B **516**, 421 (2001).
[25] M. Majumdar and A. Christine-Davis, J. High Energy Phys. 03 (2002) 056.
[26] G. Dvali and A. Vilenkin, Phys. Rev. D **67**, 046002 (2003).
[27] N. T. Jones, H. Stoica, and S. H. H. Tye, Phys. Lett. B **563**, 6 (2003).
[28] G. Dvali and A. Vilenkin, J. Cosmol. Astropart. Phys. 03 (2004) 010.
[29] E. J. Copeland, R. C. Myers, and J. Polchinski, J. High Energy Phys. 06 (2004) 013.
[30] D. N. Spergel *et al.* (WMAP Collaboration), Astrophys. J. Suppl. Ser. **148**, 175 (2003).
[31] W. J. Percival *et al.* (2dFGRS Team Collaboration), Mon. Not. R. Astron. Soc. **337**, 1068 (2002).
[32] E. Jeong and G. F. Smoot, Astrophys. J. **624**, 21 (2005).
[33] L. Pogosian, S.-H. H. Tye, I. Wasserman, and M. Wyman, Phys. Rev. D **68**, 023506 (2003).
[34] L. Pogosian, M. C. Wyman, and I. Wasserman, astro-ph/0403268.
[35] M. Wyman, L. Pogosian, and I. Wasserman, Phys. Rev. D **72**, 023513 (2005).
[36] V. M. Kaspi, J. H. Taylor, and M. F. Ryba, Astrophys. J. **428**, 713 (1994).
[37] S. E. Thorsett and R. J. Dewey, Phys. Rev. D **53**, 3468 (1996).
[38] M. P. McHugh, G. Zalamansky, F. Vernotte, and E. Lantz, Phys. Rev. D **54**, 5993 (1996).
[39] A. N. Lommen, astro-ph/0208572.
[40] F. R. Bouchet, P. Peter, A. Riazuelo, and M. Sakellariadou, Phys. Rev. D **65**, 021301(R) (2001).
[41] J. Rocher and M. Sakellariadou, Phys. Rev. Lett. **94**, 011303 (2005).
[42] M. Sazhin, M. Capaccioli, G. Longo, M. Paolillo, and O. Kovanskaya, astro-ph/0506400.
[43] M. Sazhin *et al.*, Mon. Not. R. Astron. Soc. **343**, 353 (2003).
[44] B. Linet, Ann. Inst. Henri Poincare Phys. Theor. **45**, 249 (1986).
[45] A. Vilenkin, Phys. Rev. D **23**, 852 (1981).
[46] J. R. I. Gott, Astrophys. J. **288**, 422 (1985).
[47] P. Schneider, J. Ehlers, and E. E. Falco, *Gravitational Lenses* (Springer, New York, 1992).
[48] See http://lisa.jpl.nasa.gov/.
[49] N. Seto, S. Kawamura, and T. Nakamura, Phys. Rev. Lett. **87**, 221103 (2001).
[50] See http://universe.nasa.gov/program/bbo.html.
[51] A. Albrecht and N. Turok, Phys. Rev. D **40**, 973 (1989).
[52] D. P. Bennett and F. R. Bouchet, Phys. Rev. D **41**, 2408 (1990).
[53] B. Allen and E. P. S. Shellard, Phys. Rev. Lett. **64**, 119 (1990).
[54] R. A. Matzner, Comput. Phys. **2**, 51 (1989).
[55] M. G. Jackson, N. T. Jones, and J. Polchinski, J. High Energy Phys. 10 (2005) 013.
[56] M. G. Haehnelt, Mon. Not. R. Astron. Soc. **269**, 199 (1994).
[57] R. R. Islam, J. E. Taylor, and J. Silk, Mon. Not. R. Astron. Soc. **354**, 629 (2004).
[58] K. Ioka and P. Meszaros, astro-ph/0502437.
[59] A. A. Ruffa, Astrophys. J. **517**, L31 (1999).
[60] A. Vilenkin, hep-th/0508135.
[61] X. Siemens and K. D. Olum, Nucl. Phys. **B611**, 125 (2001); **B645**, 367(E) (2002).
[62] X. Siemens, K. D. Olum, and A. Vilenkin, Phys. Rev. D **66**, 043501 (2002).